Statistical analysis of tropospheric ozone and its precursors using principal component analysis in an urban area of Surat, India

Jariwala Namrata*[1], Kapadia Drashti[1]

[1]Civil Engineering Department, Sardar Vallabhbhai National Institute of Technology, Surat, Gujarat, India

ARTICLE INFO

ABSTRACT

The objective of this study was to investigate the sources of tropospheric ozone (O_3) precursors in an urban area using principal component analysis. Chemically reactive conventional pollutants such as carbon monoxide (CO), carbon dioxide (CO_2), nitric oxide (NO), and nitrogen dioxide (NO_2), as well as some selected meteorological parameters such as global solar radiation (SR), air temperature (AT), relative humidity (RH), wind speed (WS), and wind direction (WD), were incorporated in this analysis. Real-time observation data were obtained from two monitoring stations, Limbayat and Varachha, situated in Surat city, India. The occurrence of a peak O_3 level in the summer at 5 p.m. proved the well-known fact of interconnection among the temperature, solar radiation, and increment in O_3 concentration. The potencies of CO and NO were remarkable in either the first or second principal component (PC) observed at both locations with more than 45% concentration, which alluded that the main source of O_3 was urban transportation and AT contributed with 50% weightage in the PC ascertained key role of photolysis process in the O_3 formation.

1. Introduction

Surface ozone is a colorless, reactive oxidant gas and a secondary pollutant formed from photochemically active primary pollutants. In 2009, the Indian Central Pollution Control Board (CPCB) announced revised air quality standards to control O_3 pollution, which included one-hourly (180 μg/m^3) and eight-hourly (100 μg/m^3) permissible limits for tropospheric O_3. Also, O_3 was included in the list of criteria pollutants, as prescribed by the CPCB [1]. O_3 is becoming a major concern as its concentration is increasing gradually, causing damage to plants and either directly or indirectly threatening human health even at low concentrations, as reported by Pleijel [2]. Therefore, to develop an emission control strategy, it is necessary to investigate the sources of O_3 formation, i.e., whether O_3 levels are governed by local sources (generated in the region itself) or foreign sources (transported from adjacent regions). The O_3 levels were found to be influenced by intra-urban activities and also by long-range transport [3]. In the troposphere, O_3

variation is developed by its precursors and meteorological conditions [4,5]. Along with anthropogenic emissions (fossil fuel, solvents, transport), natural sources (lightning, wetlands, forests) also contribute to O_3 precursor gases such as NO_X, CO, CH_4, and NMVOC that interact with climatic factors [6]. The role of O_3 precursors can be revealed based on O_3 formation chemistry. Sunlight (accompanied by other O_3 forming compounds) is a directly proportional factor and mostly responsible for O_3 formation, as reviewed by Lu et al. [7]. In India, huge variations are found in sunlight and temperature; therefore, the measurement dataset is distributed according to the seasons to observe its temporal variations. The temporal variability in O_3 is governed by the atmospheric process of the seasons, as characterized by Roberts-Semple et al. [8]. The information gained regarding pollutant sources and their contribution to ambient air pollution levels is known as Source Apportionment (SA) [9]. Two source apportionment models, namely positive matrix factorization and chemical mass balance, have been applied to discover the sources of particulate pollutants [10]. To identify the source contribution of aerosol, chemical characterization, temporal trends, and positive matrix factorization were performed near Houston, TX, USA [11]. Among the several types of correlation coefficients, Pearson's correlation coefficient is commonly used to measure the relationship between independent and dependent variables in linear regression and in the case of the unknown nature of the dataset. Pearson's coefficient was recently used to assess air pollutants with statistical tools in Madrid, Spain [12]. It has been used to evaluate the association between O_3 and its influencing parameters in the form of values between -1 and +1. The interpretations of 0, >0, and <0 are no association, positive association, and negative association, respectively. Here, a p value <0.01 is considered for statistical significance. Principal component analysis (PCA) is a primary tool used to screen the sources that control O_3 concentration. A large number of datasets that correlate with each other are converted to a compressed number of non-correlated and orthogonal variables that constitute a cluster, as evaluated by Martínez and Polanco [13]. PCA is used as a dimensionality reduction statistical technique in which datasets consisting of numerous interrelated variables are transformed to the most important uncorrelated new variable set, known as the principal component, with a large variance [14]. The highest possible variance occurs in the dataset represented in the first PC. In general, the size of the PC set is the same as the original dataset, and 80% of the total variance of the whole original dataset is considered in general. Standardization is used in the case of different unit measurements and where the data are measured on a large scale. According to the Kaiser criterion, PCs with an eigenvector greater than one are considered. Rotated PCs have a high impact in characterizing the potential group of non-correlated variables. The focus of this study was to investigate the potential sources of tropospheric O_3 with the help of PCA. Carbon monoxide (mg/m^3), nitrogen dioxide ($\mu g/m^3$), carbon dioxide (ppm), nitric oxide ($\mu g/m^3$), air temperature (°C), relative humidity (%), global solar radiation (W/m^2), wind direction (°), and wind speed (m/s^1) were considered as the independent variables.

2. Materials and methods

2.1. Description of the study area and instruments used

The city of Surat is situated in the western region of India on the bank of the Tapi River at a latitude of 21.1702° N and a longitude of 72.8311° E. The city has an altitude of 13.0 m from the mean sea level and covers an area of 474 km^2. Surat has a population more than 70 lacs, making it the eighth densely populated city (Census of India, 2011) in Gujarat. Real-time continuous air quality monitoring data were collected from the Surat Municipal Corporation at two locations, Limbayat and Varachha, situated at a distance of 3.6 km from each other. A continuous monitoring system was installed in both sites. The readings were recorded on an hourly basis. The monitoring point was kept on the terrace of the Surat Municipal Corporation building at the height of 15 m from the ground level in both locations. The sampling sites represent a typical urban atmosphere, surrounded by colossal roadside traffic, with an industrial area nearby. Polludrone's Continuous Ambient Air Quality Monitoring system (CAAQMS) was used to measure

the gaseous pollutants and the meteorological factors. The CO_2 was measured using the non-dispersive infra-red principle that has a 20-ppm detection limit. The CO, NO, NO_2, and O_3 were determined based on the electrochemical principle that has detection limits of 100 ppb (11.45 mg/m^3), 10 ppb (12.5 µg/m^3), 10 ppb (18.8 µg/m^3), and 10 ppb (20 µg/m^3), respectively. An ultrasonic sensor was used to measure wind speed (0–60 m/s) and wind direction (360°). The detection ranges of the respective sensors were 0 –40,000 µg/m^3 for O_3, 0–1000 µg/m^3 for $PM_{2.5}$ and PM_{10}, 0 –1000 µg/m^{-3} for CO, 0 –37,600 µg/m^3 for NO_2, 0– 52,400 µg/m^3 for SO_2, and 0– 5000 ppm for CO_2. To get higher data accuracy, an innovative e-breathing approach was adopted by the company who installed the CAAQMS system at the site. Sensor calibration for all the parameters was carried out by the manufacturer in the National Accreditation Board Laboratories; the gas calibration was done with pure air and calibration gas at a high concentration range of 1-10 ppm and flow rate of 0.5L/min before installation. As per the information available by the manufacturer of the instrument, multi-level sensor calibration was performed at a factory with

a bump test calibration facility, to test the working efficiency. Spot calibration was performed for a limited data before installation of sensors. Figure 1 shows the two monitoring locations in Surat, India, and the instrument setup at Varachha. Surat has a minimum temperature of around 10°C during the winter nights and a maximum temperature of 46°C during summer in the afternoon. Therefore, considerable variations in O_3 concentrations are found throughout the year. The diamond industries of Surat occupy about 35%– 40% of the total area (approximately 37 sq. km) of Varachha. The rest of the region is residential and commercial with heavy traffic areas. The Limbayat area is surrounded by chemical dyeing and power-loom industries, covering approximately 70% of the total area (approximately 19.6 sq. km). The textile industry emits a high pollution load in the form of CO, CO_2, NOx, and particulate matter, as reviewed by Mia et al. and Tiwari et al. [15,16].
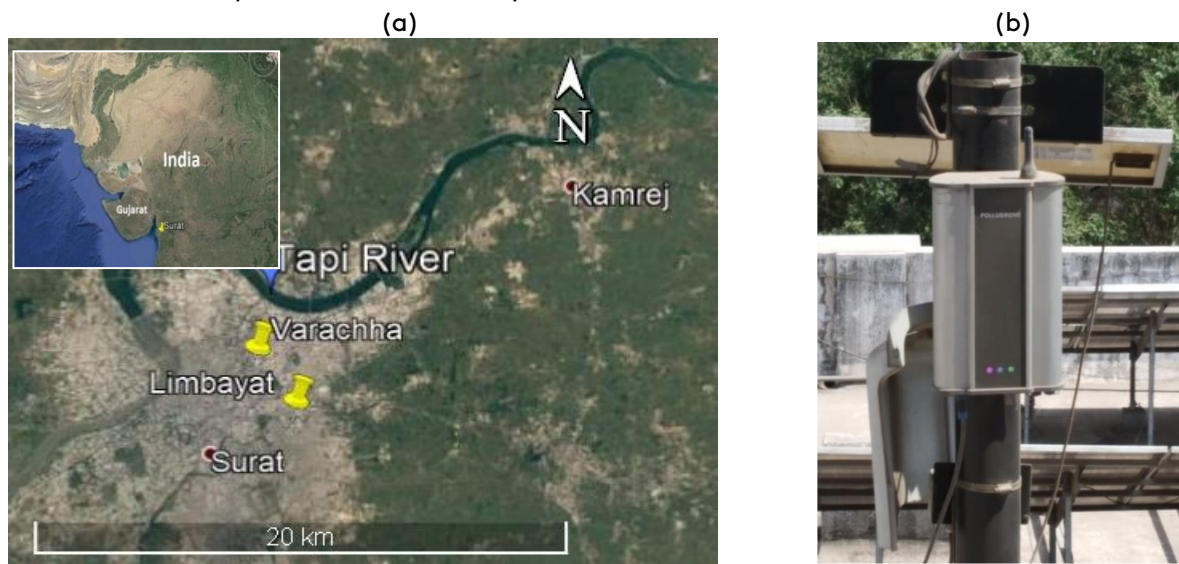
(a)	(b)

Fig.1. (a) Location of the ambient air quality monitoring stations (b) Real-time monitoring instrument setup at Varachha.

2.2. Data preprocessing

The concentrations of the above-stated parameters were recorded in the two monitoring sites from Feb 1, 2018, to Dec 14, 2019, at Limbayat and from Jan 30, 2018, to Dec 21, 2019, at

Varachha. The outlier data were removed from the O_3 data series after ascertaining that there was no occurrence of any O_3 episodic event on the corresponding day. Such events can be attributed to local photochemistry and transport [17]. In the past, research was focused on potential vorticity

(PV), which is a measure of air turbulence. PV > 1.5 (PV unit; 1 PVU = 10^{-6} km^2 $kg^{-1}s^{-1}$) in the troposphere is an indicator of stratospheric O_3 sinking; Lai et al. [18]. The global model of the European Centre for Medium-Range Weather Forecasts, using the Lagrangian method, found that the PV values at different pressure levels (300 hPa–975 hPa) change with altitude; Spreitzer et al. [19]. At the preceding and succeeding day when the highest O_3 concentration occurred, PV was <1.5 PV at all pressure levels in the 20°N–24°N latitude and 71°E–75°E longitude ranges. These data suggest the absence of the vertical transport of O_3 from the stratosphere during the corresponding days. The datasets of PV were acquired from the website: http://apps.ecmwf.int/datasets/data/interim-full-daily//; Sandhya et al. [20]. Moreover, high concentrations of O_3 were not found in the photochemically inactive hours, which indicated that there was no long-range transportation during the aforesaid days. Hence, the high concentration values of a total number of eight days were removed from the whole dataset after verifying the above criteria. During the day for the respective hour, there was low-to-moderate intensity of global SR and wind speed; hence, the photolysis process in the local region must have been responsible for the observed O_3 concentration. The missing values and non-detected (below detection limit of the particular sensor) values of the variables were found due to instrument maintenance in the entire dataset. For the missing data, the cubic spline interpolation method was applied, as suggested by Junninen et al. and Moshenberg et al. [21,22], for a 24-h diurnal cycle. The readings recorded as a below detection limit was substituted with a constant value, such as the LOD (limit of detection of the instrument) divided by the square root of 2 (thumb rule), to make the dataset reliable.

3. Results and discussion

3.1. Monthly and seasonal O_3 variations

This paper attempts to analyze the O_3 behavior in an urban area located in the industrial and commercial zone. Table 1 presents a summary of the data for O_3, as evaluated by descriptive statistics. The average hourly data for 2018 and 2019 at Limbayat and Varachha were taken for further processing. The maximum concentrations of O_3 were found in the summer season at both locations, except at Limbayat in 2019. The highest concentration was found at Limbayat in the summer of 2018 (445.22±65.53), followed by Varachha in 2018 (351.4±64.75) as shown in Table 1. The O_3 concentration in Mumbai under normal conditions (before the COVID-19 lockdown) fluctuated between 40 and 90 μg/m^3 [23]. Hourly O_3 variations can be observed by using a time-series plot, as shown in Figure 2. It indicated that hourly averaged O_3 concentrations exceeded above the threshold (180 μg/m^3) in 2018 at both locations. The data were further distributed season-wise, i.e., winter (January, February), summer (March, April, May), southwest monsoon (June, July, August, September), and post-monsoon (October, November, December), as defined by the Indian Meteorological Department, to examine the season-wise O_3 behavior.

Out of the four seasons, the maximum O_3 concentrations were observed in the summer (except at Limbayat, 2019). Therefore, to analyze further, summer diurnal variations in O_3 were compared with other independent parameters at Limbayat, as illustrated in Figure 3. The red colour O_3 concentration curve (Figure 3) depicts a strong correlation with AT in the summer. At mid-day, both concentrations reached their peak. In the morning, NO reached its maximum at about 10 a.m., indicating the high congestion in road transport. Consequently, the O_3 concentration increased in the sunlight with NO titration as per ozone photochemistry. During the night, in the absence of SR, NO_2 was not converted into NO and increased gradually, as shown in Figure 3. All these processes proved that photolysis was the governing process.

Table 1. Descriptive Statistics of O_3 ($\mu g/m^3$) at Limbayat and Varachha for 2018 and 2019.

Monitoring station	Year	Seasons	N Sample size	Number of hours for O_3 concentration more than	Max. Mg/m^3	Mean Mg/m^3	Standard deviation Mg/m^3
Limbayat	2018	Winter	576	22	381.18	51.74	58.98
		Summer	2184	118	445.22	33.74	65.53
		Southwest	4224	38	371.9	31.64	43.25
		Post-monsoon	1416	02	273.5	23.43	28.90
	2019	Winter	1152	0	130.59	25.31	26.32
		Summer	816	0	147.3	8.49	19.56
		Southwest	2880	0	105.86	8.86	11.23
		Post-monsoon	1791	0	157.39	15.53	22.83
Varachha	2018	Winter	432	21	219.7	31.04	64.35
		Summer	2208	142	351.4	41.93	64.75
		Southwest	2664	08	343.56	25.53	28.17
		Post-monsoon	1932	0	146.56	13.05	21.10
	2019	Winter	1416	0	93.72	8.16	13.99
		Summer	2208	0	101.61	5.69	13.79
		Southwest	2064	0	73.11	0.75	3.74
		Post-monsoon	1776	0	51.73	2.88	6.50

(a)   (b)
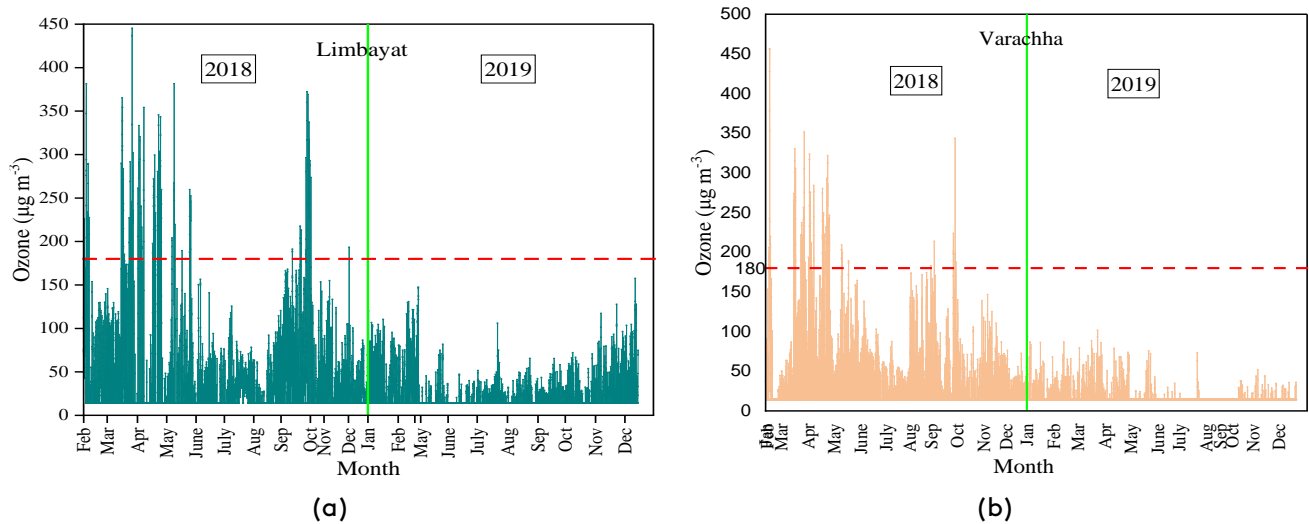
Fig. 2. Time-series plot at Limbayat and Varachha for 2018 and 2019.
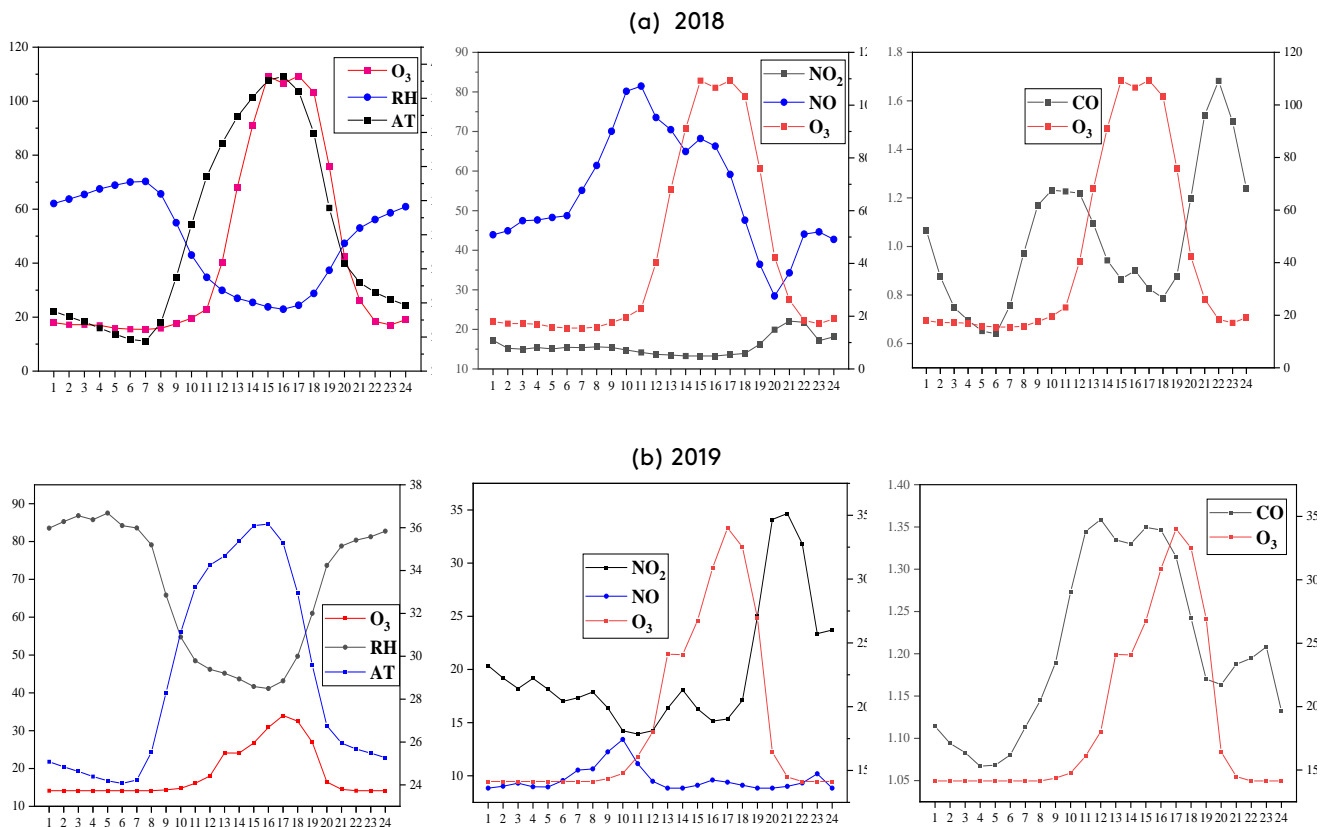
(a) 2018

(b) 2019

Fig. 3. Diurnal pattern of O_3 with RH, AT, NO, NO_2 and CO during summer at Limbayat for (a) 2018 and (b) 2019.

3.2. Correlation between O_3 and its precursors

SPSS software (version 16.0) was used to analyze the strength of the correlation between the dependent and independent variables. Pearson's correlation coefficient formula was used to establish the relationship between the variables. The formula involves the computation of the covariance of two variables that are divided by the standard deviation of each measurement.

$$r_{xy} = \frac{\sum_{i=1}^{n}(x_i - \overline{x})(y_i - \overline{y})}{\sqrt{\sum_{i=1}^{n}(x_i - \overline{x})^2}\ \sqrt{\sum_{i=1}^{n}(y_i - \overline{y})^2}} \qquad (1)$$

Table 2 shows that the correlation coefficient has a value >0.4 (|r| > 0.4) between O_3 and CO, NO_2, CO_2, NO, AT, RH, SR, WD, and WS during the four seasons at Limbayat and Varachha. The positive relationship between O_3 and AT and the strong and moderately inverse relationship with RH in most of the seasons indicate that the source of O_3 is mainly the photochemical processes of the primary pollutants.

Table 2. Pearson's correlation coefficient (r) between O_3 and conventional air pollutants along with the meteorological parameters (|r| > 0.4).

Winter							
Limbayat				Varachha			
2018		2019		2018		2019	
AT	0.468	AT	0.499	CO	0.463	AT	0.475
RH	-	RH	-				
Summer							
Limbayat				Varachha			
2018		2019		2018		2019	
AT	0.654	CO	0.476	AT	0.579	-	-
RH	-	AT	0.583	RH	-		
		RH	-				
Southwest monsoon							
Limbayat				Varachha			
2018		2019		2018		2019	
-	-	-	-	NO	-	-	-
Post-monsoon							
Limbayat				Varachha			
2018		2019		2018		2019	
-	-	-	-	CO_2	-	-	-
				RH	-		

Note: (-) indicates correlation coefficient values <0.4.
The correlation values mentioned in the table are significant at the 0.01 level (2-tailed).

3.3. PCA on multivariate data

In this method, ten correlated elements were transformed into PCs. The total variance of the PCs was the same as the variance of the original variables. The PCs were arranged from the highest to the lowest. The first PC (PC1) represented the major variance in the data, and the tenth PC (PC10) had the lowest variance [24].

In this study, PCA functioned in the following way:

$$PCi = \sum_{i=1}^{n} v_{ki}x_i \qquad (2)$$

where x_i is the original element in the dataset and v_{ki} is the eigenvector. The PCA coefficients were calculated with the help of the correlation matrix, identity matrix, and eigenvalue. The PC scores obtained from the summation of the products of the original variables' value and their loadings were utilized for further interpretation. PCA was performed using the R open access software along with packages such as FactomineR and FactoInvestigate. The Varimax function was used for rotating the components toward their principal axes to develop the rotated factor loadings. PCA was applied to ten different variables seasonally to analyze the dependence of O_3 concentration on other variables. The first two PCs of all the variables were used owing to high variances, as shown in Table 3. The results obtained from the PCA, correlation study, and a previous research paper (based on the chemical reaction involved in O_3 formation) have been included to identify the primary source of the secondary pollutant O_3. As seen in Table 4, the release of CO moderately and strongly influenced the increment of O_3 throughout the year in both 2018 and 2019 at Limbayat.

Table 3. First two PCs of all elements for 2018 and 2019.

	Winter							
	Limbayat				Varachha			
	2018		2019		2018		2019	
Elements	PC1	PC2	PC1	PC2	PC1	PC2	PC1	PC2
CO	-0.046	0.895	-0.033	0.838	0.315	-0.437	0.771	-0.139
NO_2	0.042	0.112	-0.755	-0.108	-0.066	0	0.207	-0.737
O_3	0.848	-0.134	-0.013	0.105	0.588	0.312	0.426	-0.179
CO_2	-0.046	0.03	0.02	-0.192	-0.111	0.118	0.054	-0.053
NO	0.287	0.394	0.203	0.88	0.101	-0.063	0.768	0.35
AT	0.715	0.086	0.736	-0.046	0.9	0.03	0.296	0.528
RH	-0.691	-0.366	-0.277	-0.436	-0.814	0.307	-0.828	-0.047
Solar	0.386	0.147	0.799	0.142	0.74	0.201	0.428	0.746
WD	-0.457	-0.464	0.132	-0.092	-0.272	0.472	-0.248	0.012
WS	0.013	-0.141	0.043	-0.106	0.12	0.863	-0.105	0.106

In most urban areas, aerosol and CO are the leading gases emitted from gasoline fueled vehicles [25]. During 2007–2017, more than 28.87 lakh motor vehicles were registered in Surat City; it is the fastest growing city in the last ten years, followed by Kanpur and Pune [26]. Emission inventory was done in Bengaluru in 2015, and it was observed that vehicular exhaust contributed to 70.7% of the CO emission [27]. Regarding the season-wise formation of the PCs, CO and NO were found in a group either by PC1 or PC2 in most of the seasons. Hence, it could be stated that the main source of O_3 precursor was vehicular exhaust. In the summer season (Table 4) at Limbayat, O_3 was grouped with CO and CO_2 along with AT and RH in 2019. Furthermore, particulate matter, nitrogen oxide, CO, and hydrocarbons are vehicle criteria pollutants [28]. In the commercial area of Varachha, WD and WS played important roles (Table 4). Hence, O_3 levels can be controlled by equipping the vehicle engines with the latest technologies. On the other hand, the Centre for Science and Environment reported increased levels of O_3 during the COVID-19 lockdown in 22 cities across India even though it flattened the NO_2 curve [29]. The data were unavailable for March and April in 2019 at Limbayat, owing to instrument maintenance.

Table 4. Summary of the variables with the highest contribution in the first two PCs.

Limbayat															
Winter				Summer				Southwest monsoon				Post-monsoon			
2018		2019		2018		2019		2018		2019		2018		2019	
PC1	PC2	PC1	PC2	PC1	PC2	PC1	PC2	PC1	PC2	PC1	PC2	PC1	PC2	PC1	PC2
O_3	NO	WS	CO	O_3	CO	CO	SR	AT	WD	NO_2	CO	AT	NO	NO_2	CO_2
AT	CO	NO	NO_2	AT	NO	O_3		RH	WS	AT	NO	RH	WS	NO	O_3
RH		O3		RH	WD	CO_2	NO_2	SR	CO	RH		SR	NO_2	AT	
WD		AT		SR		AT			NO	SR			O_3	RH	
WS		RH		WS		RH			CO_2					SR	
		SR				SR									

Varachha															
Winter				Summer				Southwest monsoon				Post-monsoon			
2018		2019		2018		2019		2018		2019		2018		2019	
PC1	PC2	PC1	PC2	PC1	PC2	PC1	PC2	PC1	PC2	PC1	PC2	PC1	PC2	PC1	PC2
NO_2	CO	CO	CO_2	O3	CO_2	CO	CO_2	AT	CO	NO	O3	CO	O_3	NO	NO_2
AT	O_3	NO	WS	AT	CO	NO	WS	RH	CO_2	AT	NO_2	NO	CO_2	AT	WD
RH		AT		RH	NO	AT	WD	SR	WS	RH		AT		RH	WS
SR		RH		SR		RH			SR			SR	RH	SR	
		SR		WS		SR									

4. Conclusions

In this research work, the O_3 concentration variations with seasons were analyzed at two locations, Varachha and Limbayat of Surat city. With PC variable loadings, the relationship of O_3 with other pollutants, and several meteorological factors were investigated. In a seasonal diurnal pattern, a higher concentration of surface O_3 was observed during the daytime, especially afternoon or early evening, when compared with the nighttime due to the higher temperature. In the entire year, the maximum O_3 concentration was noted in the summer, owing to the influence of meteorological parameters such as AT and SR. This result was also proven by the moderate correlation coefficient between tropospheric O_3 and temperature in the summer season at both locations. In the PC variable loadings, the group of NO and CO in the first or second PC revealed the effect of the local source, i.e., road transport is the main source. The meteorological factors with O_3 in the same cluster disclosed the presence of photochemical reactions of ozone. Conclusively, in the numerical or chemical source apportionment of ozone, PCA can be used as an effective pre-processor tool.

Acknowledgments

References

[1] Kamyotra, S. J. S., Saha, D., Tyagi, S. K., Sen, A. K., Srivastava, R. C., Pathak, A. (2011). Guidelines for the measurement of ambient air pollutants.1–7

[2] Pleijel, H. (1999). Ground-Level Ozone – A Threat to Vegetation. *Swedish Environmental protection agency.*

[3] Mukherjee, A., Agrawal, S. B., Agrawal, M. (2018). Intra-urban variability of ozone in a tropical city—characterization of local and regional sources and major influencing factors. *Air quality, atmosphere and health, 11(8)*, 965–977.

[4] Marathe, S. A., Murthy, S. (2015). Seasonal Variation in Surface Ozone Concentrations, Meteorology and Primary Pollutants in Coastal Mega City of Mumbai, India. *Journal of climatology and weather forecasting, 03(03)*, 1–10.

[5] Chattopadhyay, G., Midya, S. K., Chattopadhyay, S. (2021). Information Theoretic Study of the Ground-Level Ozone and Its Precursors Over Kolkata, India, During the

Summer Monsoon. *Iranian journal of science and technology, transaction A: science, 45(1),* 201–207.

[6] Fowler, D., Amann, M., Anderson, R., Ashmore, M., Cox, P., Depledge, M., Derwent, D., Grennfelt, P., Hewitt, N., Hov, O., Jenkin, M. (2008). Ground-level ozone in the 21st century: future trends, impacts and policy implications. *The royal society,* *https://royalsociety.org/topics-policy/publications/2008/ground-level-ozone.*

[7] Lu, X., Zhang, L., Shen, L. (2019). Meteorology and climate influences on tropospheric ozone: a review of natural sources, chemistry, and transport patterns. *Current pollution reports, 5(4),* 238–260.

[8] Roberts-Semple, D., Song, F., Gao, Y. (2012). Seasonal characteristics of ambient nitrogen oxides and ground-level ozone in metropolitan northeastern New Jersey. *Atmospheric pollution research, 3(2),* 247–257.

[9] Belis, C. a, Larsen, B. R., Amato, F., Haddad, I. El, Favez, O., Harrison, R. M., Hopke, P. K., Nava, S., Paatero, P., Prévôt, A., Quass, U., Vecchi, R., Viana, M. (2014). European guide on air pollution source Apportionment with receptor models. EUR Luxembourg (Luxembourg): Publications Office of the European Union.

[10] Shi, G., Liu, J., Wang, H., Tian, Y., Wen, J., Shi, X., Feng, Y., Ivey, C. E., Russell, A. G. (2018). Source apportionment for fine particulate matter in a Chinese city using an improved gas-constrained method and comparison with multiple receptor models. *Environmental pollution, 233,* 1058–1067.

[11] Sheesley, R. J. ed. (2018). Air Quality and Source Apportionment. *MDPI AG-multidisciplinary digital publishing institute.*

[12] Núñez-Alonso, D., Pérez-Arribas, L. V., Manzoor, S., Cáceres, J. O. (2019). Statistical Tools for Air Pollution Assessment: Multivariate and Spatial Analysis Studies in the Madrid Region. *Journal of analytical methods in chemistry, 1-9.*

[13] Polanco Martínez, J. M. (2016). The role of principal component analysis in the evaluation of air quality monitoring networks 1

Introduction. *Comunicaciones en estadística, 9(2),* 255–277.

[14] Bartholomew, D. J. (2010). Principal components analysis. International encyclopedia of education, 374–377.

[15] Mia, R., Selim, M., Shamim, A. M., Chowdhury, M., Sultana, S., Armin, M., Hossain, M., Akter, R., Dey, S., Naznin, H. (2019). Review on various types of pollution problem in textile dyeing and printing industries of Bangladesh and recommandation for mitigation. *Journal of textile engineering and fashion technology, 5(4),* 220–226.

[16] Tiwari. M., Babel.S. n.d. (2013). Air pollution in textile industry. *Asian journal of environmental science, 8(1),* 64–66.

[17] Verma, N. 2018. An investigation of ozone formation through its precursors (CO; NOx; VOC) and its loss processes at a sub-urban site of agra. *Dayalbagh educational institute.*

[18] Lai, T. L., Talbot, R., Mao, H. (2012). An investigation of two highest ozone episodes during the last decade in New England. *Atmosphere, 3(1),* 59–86.

[19] Spreitzer, E., Attinger, R., Boettcher, M., Forbes, R., Wernli, H., Joos, H. (2019). Modification of potential vorticity near the tropopause by nonconservative processes in the ECMWF model. *Journal of the atmospheric sciences, 76(6),* 1709–1726.

[20] andhya, M., Sridharan, S., Indira Devi, M., Gadhavi, H. (2015). Tropical upper tropospheric ozone enhancements due to potential vorticity intrusions over Indian sector. *Journal of atmospheric and solar-terrestrial physics, 132,* 147–152.

[21] Junninen, H., Niska, H., Tuppurainen, K., Ruuskanen, J., Kolehmainen, M. (2004). Methods for imputation of missing values in air quality data sets. *Atmospheric environment, 38(18),* 2895–2907.

[22] Moshenberg, S., Lerner, U., Fishbain, B. (2015). Spectral methods for imputation of missing air quality data. *Environmental systems research, 4(26)* 1-13.

[23] Korhale, N., Anand, V., Beig, G. (2021). Disparity in ozone trends under COVID-19 lockdown in a closely located coastal and hillocky metropolis of India. *Air quality,*

atmosphere and health, 14(4), 533–542.

[24] Huang, R. J., Zhang, Y., Bozzetti, C., Ho, K. F., Cao, J. J., Han, Y., Prévôt, A. S. (2014). High secondary aerosol contribution to particulate pollution during haze events in China. *Nature*, *514*(7521), 218–222.

[25] Larsen, R. I. (1966). Air pollution from motor vehicles. *Annals of the New York academy of sciences, 136(12),* 277–301.

[26] Transport research wing of the ministry of road transport and highways. 2019. *The road transport year book*. New Delhi.

[27] Guttikunda, S. K., Nishadh, K. A., Gota, S., Singh, P., Chanda, A., Jawahar, P., Asundi, J. (2019). Air quality, emissions, and source contributions analysis for the Greater Bengaluru region of India. *Atmospheric pollution research*, *10*(3), 941-953.

[28] Winkler, S. L., Anderson, J. E., Garza, L., Ruona, W. C., Vogt, R., Wallington, T. J. (2018). Vehicle criteria pollutant (pm, no x, co, hcs) emissions: how low should we go?. *Npj Climate and atmospheric science*, *1*(1), 1-5.

[29] Reports. (2020). Air quality analysis during summer lockdown : Some highlights. *Centre for Science and Environment (CSE)* .